Interfacial Behavior of Ferrocene- and 1,4-Naphthoquinone-based Compounds, and Their Mixtures with Monoolein at the Air/Water Interface

Daiva Tauraitė[a], Valdemaras Razumas[a], Tommy Nylander[b], and Eugenijus Butkus[c]

[a] Department of Bioelectrochemistry and Biospectroscopy, Institute of Biochemistry, Mokslininkų 12, LT-08662 Vilnius, Lithuania
[b] Department of Physical Chemistry 1, Center for Chemistry and Chemical Engineering, Lund University, P.O. Box 124, S-221 00 Lund, Sweden
[c] Department of Organic Chemistry, Vilnius University, Naugarduko 24, LT-03225 Vilnius, Lithuania

Reprint requests to Daiva Tauraitė. Fax: +370-5-2729196. E-mail: daivat@bchi.lt

Z. Naturforsch. **2008**, *63b,* 1093 – 1100; received June 9, 2008

In this work, a study of the interfacial properties of redox-active novel ferrocene- and 1,4-naphthoquinone-based compounds containing an alkenyl chain is presented. The miscibility of these compounds with 1-monooleoylglycerol (monoolein, MO), a well-known and much studied substance because of its rich polymorphism in water, at the air/water interfaces was investigated by using the Langmuir surface film balance to get a better understanding of the interaction between MO and the new derivatives. The influence of temperature on the monolayer structure was also studied. It has been demonstrated that the monolayers of all compounds have a liquid-expanded structure, and that the mixed films are more stable compared to the layers of the individual compounds.

Key words: Monolayers, Air/Water, Redox-active Compounds, Ferrocene, 1,4-Naphthoquinone

Introduction

The spreading of amphiphilic molecules with poor water solubility at the air/aqueous interface, and the question whether particular amphiphiles form stable monomolecular films or not have been investigated since the days of Franklin [1] and Pockels [2]. Monolayers have a wide range of applications including optical devices, biological sensors and models for biological membranes [3]. These 2D-systems are also extensively used to monitor enzymatic reactions at interfaces, *e. g.* enzyme-catalyzed lipolytic processes [4]. For this purpose, the properties of layers formed by spreading of a very wide variety of substances, like triglycerides and their derivatives, vitamins, sterols, redox-active ferrocene derivatives, porphyrins and polymers, not to mention fatty acids and phospholipids and sphingomyelins, at the air/water interface have been investigated [1, 5 – 11]. The interaction between DNA and cationic lipid monolayers at the air/water interface has also been widely investigated [12, 13]. The development of new techniques, such as X-ray diffraction measurements [14], ellipsometric microscopy [15], and, more recently, Brewster angle microscopy (BAM) [16] and atomic force microscopy (AFM) [17, 18], grazing-incidence X-ray diffraction (GIXD) and X-ray specular reflectivity [19, 20], and fluorescence microscopy [5, 21, 22] has made it possible to determine the micro- and nanoscopic organization of amphiphilic substances in the monolayer. In many cases, the surface film balance can also give sufficient information on whether or not a compound forms a stable monolayer, on the area per molecule, the miscibility of the amphiphiles in the monolayer as well as the monolayer phase behavior.

In general terms, our prime research interest is in the development of lipid-based aqueous liquid-crystalline phases as matrices for enzyme immobilization [23]. In the special case where the entrapped enzyme belongs to the oxidoreductase class, the incorporation of redox-active amphiphiles into the lipid-based matrix might promote the electron transfer between the enzyme's active center and the matrix [24, 25]. On the other hand, it should also be mentioned that in nature certain enzymes, *e. g.* the enzymes of the respiratory chain, are only active in the presence of membrane-bound redox cofactors like ubiquinone.

The purpose of providing the synthetic redox-active compounds as lipid matrix components is to get a han-

0932–0776 / 08 / 0900–1093 $ 06.00

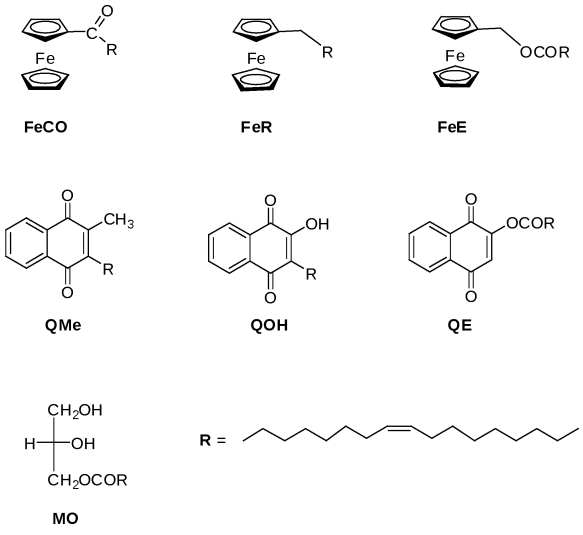

Fig. 1. Structures of ferrocene and 1,4-naphthoquinone compounds and monoolein (MO).

dle on how miscible a particular type of derivatives is with the lipids in the matrix. Based on these findings, transducer molecules that preserve a certain polymorphic lipid structure can be designed.

In this work, the results of a study of the interfacial properties of some novel ferrocene and 1,4-naphthoquinone derivatives (Fig. 1) at the air/water interface are presented. The miscibility of these compounds with 1-monooleoylglycerol (monoolein, MO), which exhibits rich polymorphism in water [26], at the interface was investigated by using the surface film balance to get a better understanding of the interaction between MO and the new derivatives.

An interesting application of these types of redox-active compounds, which also show marked absorption bands in the vibrational spectra, has been demonstrated by Niaura *et al.* [27]. The authors used infrared-visible sum-frequency-generation (SFG) vibrational spectroscopy to probe the activity of *Thermomyces lanuginosus* lipase at the air/water interface. As a self-assembling substrate, the authors used the ester compound *O*-palmitoyl-2,3-dicyanohydroquinone, which has structural similarities with the QE compound used in the present study (see Fig. 1).

Experimental Section

Materials

Monoolein [1-mono(*cis*-9-octadecenoyl) glycerol, MO], > 99 % pure, lot nr. M-239-JA21-I, was obtained from Nu Chek Prep Inc. (Elysian, MN).

Ferrocene derivatives: ferrocenylmethyl (*Z*)-octadec-9-enoate (FeE), ((*Z*)-octadec-9-enoyl)ferrocene (FeCO) and ((*Z*)-octadec-9-enyl)ferrocene (FeR) (for structures, see Fig. 1) were synthesized as described previously [28].

Synthetic procedures

2-((Z)-heptadec-8-enyl)-3-methyl 1,4-naphthoquinone (QMe) and 2-((Z)-heptadec-8-eny)-3-hydroxy-1,4-naphthoquinone (QOH)

To 2-methyl-1,4-naphthoquinone (1 g, 5.8 mmol) or 2-hydroxy-1,4-naphthoquinone (1 g, 5.7 mmol) in 40 mL of acetonitrile or acetonitrile and water (1/1 volume ratio), respectively, oleic acid (1.4 g, 5.0 mmol) and silver nitrate (0.5 g, 3.0 mmol) were added and heated to 60 °C until complete dissolution. To this mixture, a solution of ammonium persulfate (2.28 g, 10.0 mmol) in 15 mL of water was added while stirring. After heating the mixture at 60 – 65 °C for 50 min, the mixture was cooled, and the product was extracted with chloroform. After washing with saturated aqueous solutions of sodium bicarbonate and sodium chloride and several times with water, the product was purified by column chromatography (silica gel, eluent chloroform/hexane) yield 0.95 g or 0.5 g (25 – 47 %), respectively.

QMe: ^{1}H NMR (500 MHz, $CDCl_3$): δ = 0.87 (t, 3 H, CH_3), 1.28 – 2.62 (m, 28 H, CH_2), 2.18 (s, 3 H, CH_3), 5.34 (t, 2 H, CH=), 7.72 – 8.00 (dd, 4 H, C_6H_4). – $C_{28}H_{40}O_2$: calcd. C 82.30, H 9.87; found C 82.02, H 9.41.

QOH: ^{1}H NMR (500 MHz, $CDCl_3$): δ = 0.86 (t 3 H, CH_3), 1.25 – 2.59 (m, 28 H, CH_2), 5.33 (t, 2 H, CH=), 7.75 – 8.06 (dd, 4 H, C_6H_4). – $C_{27}H_{38}O_3$: calcd. C 78.98, H 9.33; found C 78.68, H 9.78.

((Z)-Octadec-9-enyl) 1,4-naphthoquinone-2-carboxylate (QE)

To a solution of 2-hydroxy-1,4-naphthoquinone (2 g, 11.4 mmol) in a mixture of acetonitrile and methylene chloride (80 mL, 1/1 volume ratio) containing 0.8 g (10.0 mmol) of sodium carbonate, oleoyl chloride (3.3 mL, 10.0 mmol) was added. After stirring for 2 h at r.t. the solvents were evaporated. The residue was dissolved in chloroform, washed with water and purified by column chromatography (silica gel, eluent chloroform/hexane), yield 0.5 g (23 %). – ^{1}H NMR (500 MHz, $CDCl_3$): δ = 0.88 (t, 3 H, CH_3), 1.28 – 2.65 (m, 28 H, CH_2), 5.35 (t, 2 H, CH=), 6.74 (t, 1 H, CH=), 7.81 – 8.06 (dd, 4 H, C_6H_4). – $C_{28}H_{38}O_4$: calcd. C 76.68, H 8.73; found C 76.77, H 8.65.

Methods

The ^{1}H NMR spectra were recorded at 300 MHz on a Varian Unity Inova 300 spectrometer in $CDCl_3$. The NMR chemical shifts are expressed in δ (ppm) relative to hexamethyldisiloxane as internal standard. The purity of the syn-

thesized compounds was proved by GC-MS, spectroscopic methods and elemental analysis.

The monolayer structural characteristics were studied by measuring the π-*A* (surface pressure *vs*. area per molecule) isotherms using a surface film balance type 611 from Nima Technology (Coventry, England). The surface film was formed by spreading 1,4-naphthoquinone- and ferrocene-based compounds, and their mixtures with monoolein as solutions using hexane as a spreading solvent. Analytical grade hexane was used without further purification. The water used as sub-phase was ion-exchanged, distilled, and passed through a milli-Q water purification system (Bedford, MA). The compression rate is critical when the monolayer is not stable. In this work, the isotherms were recorded at a compression speed of 60 $cm^2\,min^{-1}$, although no effect of compression speed in the range of 40 – 100 $cm^2\,min^{-1}$ was observed. Collapse of the MO monolayer was not observed with a barrier speed of 20 $cm^2\,min^{-1}$. The film balance was calibrated before each measurement. The air/water interface was cleaned by sweeping the interface with the Teflon barrier and aspirating the surface to remove any contamination from the compressed film. This was repeated until the value of the surface pressure was the same as the literature value for pure water, and the surface pressure increase upon maximum compression was less than 0.1 $mN\,m^{-1}$. For the spreading of the mixtures, the components were dissolved individually in the spreading solvent and then premixed in the required ratio. Aliquots of 60 – 70 μL solutions were spread at the air/water solution interface at 20 °C using a microsyringe. Compression was started after a film equilibration time of 10 min. The experiments were repeated at least twice confirming good reproducibility of the data obtained.

Results and Discussion

Generally, the π-*A* (surface pressure *vs.* area per molecule) isotherm features the transition from gaseous to liquid (expanded and condensed) and then to solid 2D-phases with increasing pressure [29], depending on the particular amphiphile, sub-phase and temperature [30]. The phase transitions of monolayers formed from mixtures of amphiphiles can be obscured by non-ideal mixing and lateral phase separation leading to the formation of separate domains [31]. Another factor that might complicate the interpretation of the π-*A* isotherm is the instability of the formed monolayer. This makes the π-*A* isotherm dependent on the compression speed, in that the observed area per molecule is significantly less than expected from the molecular dimensions and usually decreases with the compression speed. It is important to bear in mind that, even though the amphiphile that makes up the monolayer has very low solubility, the monolayer formed at the air/aqueous interface can be meta-stable. Apart from processes such as rearrangement of the amphiphiles or dissolution into the sub-phase, a transformation to a three-dimensional phase can occur at pressures above the equilibrium spreading pressure [32, 33]. Furthermore, the stability of the monolayers is very much dependent on the solvent and the techniques used for spreading the lipid [34], and also on the conformation of the head group of the lipid [35].

In this work, the π-*A* isotherm for spread monoolein (MO) was initially investigated at different compression rates in order to establish under which conditions the monolayer is stable enough to record the isotherm. At compression rates below 40 cm^2/min, the isotherms were shifted towards a smaller area per molecule, and the collapse of the MO monolayer could not be observed at a barrier speed of 20 cm^2/min. Therefore, it is clear that the MO monolayers are meta-stable, as has been reported earlier [36, 37]. Such behavior can be related to the fact that MO, in an excess of water, forms 3D-structures with reversed curvature, *i. e.* the bicontinuous cubic phase [26]. In fact, studies of the relaxation of MO monolayers close to the collapse at π of about 46 mN/m indicate that the process could be considered to occur prior to the formation of mesomorphic phases close to the interface [37]. In addition, the desorption of MO, which is believed to be the dominating factor for the relaxation below the equilibrium spreading pressure ($\pi_e \approx 46$ $mN\,m^{-1}$ [38]), also contributes to the relaxation process at this high pressure. It has also been reported that the MO monolayer shows weak X-ray diffraction, even at high surface pressures (π = 35 $mN\,m^{-1}$), confirming a low degree of organization within the layer [39]. The lack of a defined structure within the MO monolayer has also been observed by BAM studies [40]. The interfacial layer of MO is also thin, *ca.* 13 Å, where the thickness of the acyl chain region is about 9.3 Å [39]. However, it should be noted that we did not observe any effect of compression speed on the π-*A* isotherms in the range of 40 – 100 $cm^2\,min^{-1}$. Therefore, the isotherms in the present study were recorded at a compression speed of 60 cm^2/min.

π-A Isotherms for the pure ferrocene- and 1,4-naphthoquinone-based compounds

The π-*A* isotherms for the ferrocene and 1,4-naphthoquinone derivatives of Fig. 1 are shown in Figs. 2 and 3, respectively.

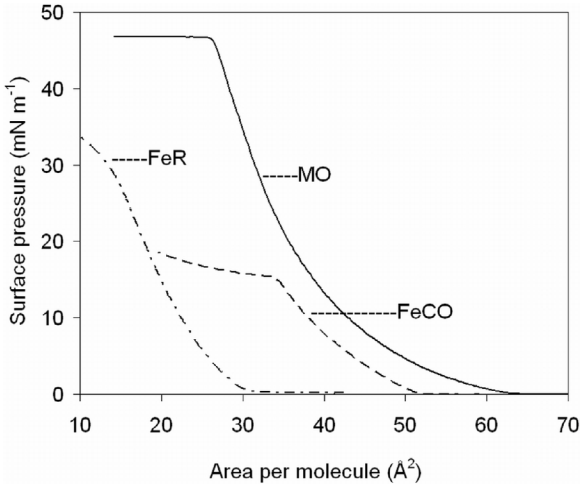

Fig. 2. Surface pressure-area isotherms for spread films of monoolein (MO) and the ferrocene derivatives ((*Z*)-octadec-9-enoyl)ferrocene (FeCO) and ((*Z*)-octadec-9-enyl)ferrocene (FeR) at the air/water interface at 20 °C.

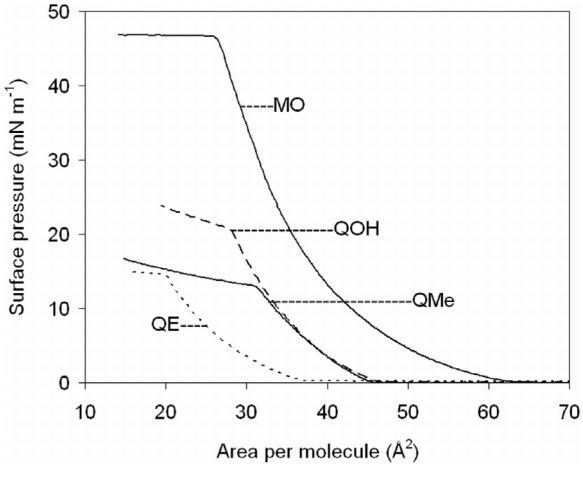

Fig. 3. Surface pressure-area isotherms for spread films of monoolein (MO) and the 1,4-naphthoquinone derivatives 2-((*Z*)-heptadec-8-enyl)-3-methyl 1,4-naphthoquinone (QMe), 2-((*Z*)-heptadec-8-enyl)-3-hydroxy-1,4-naphthoquinone (QOH), and ((*Z*)-octadec-9-enyl) 1,4-naphthoquinone-2-carboxylate (QE) at the air/water interface at 20 °C.

For comparison, the π-*A* isotherm recorded for MO is also shown. The isotherm for MO corresponds well to the previously published isotherms [36, 40] and shows only a liquid expanded structure. We observed a collapse pressure of about 47 mN m^{-1}, which is slightly higher than reported earlier [36, 40]. The π-*A* isotherms for all the other compounds are shifted towards smaller areas per molecule compared to the isotherm recorded for MO. This apparent smaller area per molecule for ferrocene and 1,4-naphthoquinone derivatives, compared with pure MO, can be due to more efficient packing at the interface, possibly caused by stronger interaction between the ferrocene and naphthoquinone head groups. However, poor spreadability of the compounds and/or poor stability of the formed monolayers can also cause smaller *A* values, which is also indicated by the much lower collapse pressure for the derivatives. Based on the molecular structure, one would also expect that the studied derivatives might be less surface active compared to MO. In particular, the ferrocenes seemed to be harder to spread than the 1,4-naphthoquinone-based compounds. One of the ferrocene compounds, ferrocenylmethyl (*Z*)-octadec-9-enoate (FeE), was impossible to spread quantitatively. No increase in surface pressure was observed upon compression, even after very long equilibrium times (hours) after spreading.

The ((*Z*)-octadec-9-enyl)ferrocene (FeR) appeared also more difficult to spread than the other compounds studied. Long equilibration times (about 1 h) were needed after spreading before a reproducible isotherm could be recorded. When a shorter equilibration time was applied, the compression isotherm recorded after a compression-expansion cycle was shifted to an apparently larger *A*. This suggests that the spreading from hexane resulted in a formation of aggregates, which, given enough time, were dissolved into a more or less homogeneous monolayer. Consequently, allowing for 1 h equilibration time after spreading, gave identical π-*A* isotherms after each compression-expansion cycle. The area per molecule recorded at collapse is the smallest of all derivatives confirming the strong intermolecular interactions. It is likely that aggregates of FeR still remain at the surface, hence the unexpectedly low surface area. FeR is also likely to be the most hydrophobic of the ferrocene compounds.

The collapse pressure decreases in the order MO > FeR > FeCO. It should be noted that the observed plateau for FeCO can also be interpreted as a phase transition and not a collapse, as will be discussed further below. The areas per molecule for the 1,4-naphthoquinone derivatives QMe and QOH were the same, while for QE the parameter was shifted to a lower value. This is not surprising as QMe and QOH have quite similar structures. However, QOH is expected to be more amphiphilic as it has an –OH group instead of the methyl group in QMe. This shows up as a

higher collapse pressure for the former compound. For the 1,4-naphthoquinone-based derivatives, the parameter decreases in the order MO > QOH > QE > QMe.

The effect of temperature on the monolayer structure

To further investigate the properties of the spread monolayer, the π-*A* isotherms for some of the derivatives were recorded at different temperatures in the range of 15 – 30 °C. The effect of temperature on the π-*A* isotherms of monoglyceride (monostearin, MO, monopalmitin) monolayers is well-documented in the literature [41 – 43]. Monostearin presents a rich structural polymorphism – solid, liquid-condensed or liquid-expanded structures are possible depending on the temperature and on the molecular area [41]. The π-*A* isotherm of MO is more featureless and shows that the layer is liquid-expanded independent of the temperature in the range of 10 – 40 °C [36, 42]. The isotherms are shifted towards larger areas per molecule with increasing temperature [36, 43], while the collapse pressure decreases slightly with increasing temperature [42]. An expansion of the monolayer with increasing temperature could be explained as an effect of the increased mobility of the acyl chains of MO.

The π-*A* isotherms for the 1,4-naphthoquinone derivatives (data not shown) were shifted towards smaller *A* values with increasing temperature. Such a decrease in area per molecule with temperature could be attributed to loss (desorption) of the spread substance to the sub-phase due to an increase of solubility with temperature [37]. The collapse pressure, however, did not change with temperature. The effect of the temperature on the π-*A* isotherms was generally higher for the ferrocene derivatives compared to the naphthoquinones (Figs. 4 and 5).

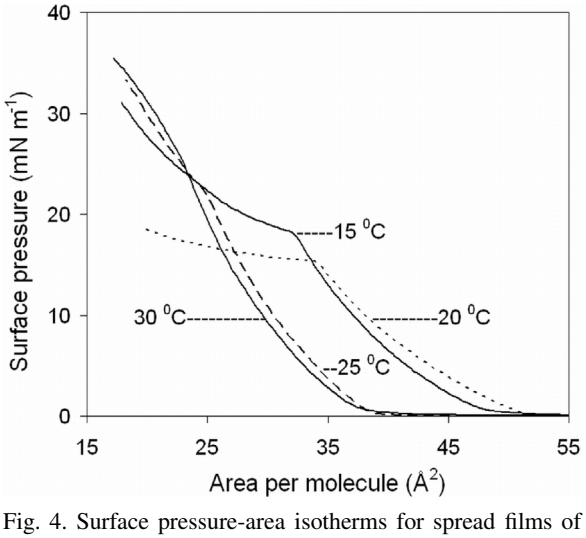

Fig. 4. Surface pressure-area isotherms for spread films of ((*Z*)-octadec-9-enoyl)ferrocene (FeCO) at the air/water interface at different temperatures between 15 and 30 °C.

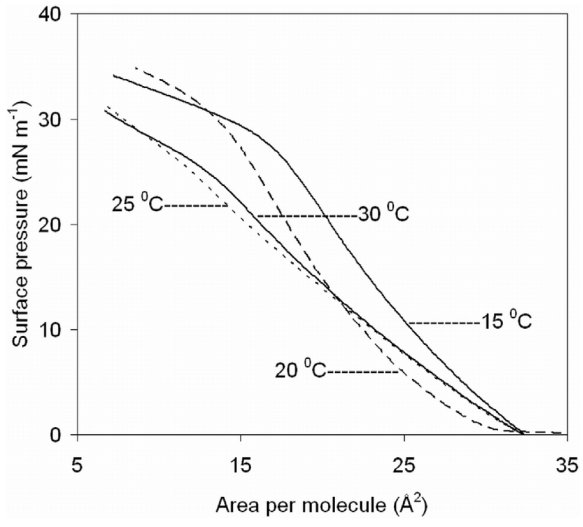

Fig. 5. Surface pressure-area isotherms for spread films of ((*Z*)-octadec-9-enyl)ferrocene (FeR) at the air/water interface at different temperatures between 15 and 30 °C.

In particular for the FeCO derivative, there is a drastic change in the isotherm between 20 and 25 °C. At 25 and 30 °C, the isotherm looks like the one for a monolayer in a liquid-expanded state. The π-*A* isotherm at 20 °C features a plateau, which can be interpreted as a collapse or a transition from a liquid-expanded to a liquid-condensed phase. Since the plateau disappears with increasing temperature, the phenomenon is most likely due to a phase transition. Thus, π-*A* isotherms of FeCO at different temperatures bear a resemblance to those recorded for, *e. g.*, monopalmitin, where the liquid-expanded – liquid-condensed phase transition disappears at high temperature [42].

The liquid-expanded liquid-condensed phase transition seems to occur at higher pressure, when the temperature is decreased from 20 to 15 °C (Fig. 4). The area per molecule of FeCO is decreasing with temperature as expected. This implies more crystalline chains and possibly a slightly different orientation of the amphiphile at the interface. It is possible that such a different orientation can affect the pressure at which a phase transition occurs. The area per FeR molecule seems to decrease with increasing temperature (Fig. 5), which

can be explained by an increasing loss of material to the sub-phase. Furthermore, this compound was hard to spread quantitatively as discussed above.

π-A Isotherms for mixtures with monoolein

The miscibility of the synthesized derivatives with MO at the air/water interface was investigated by recording the *π-A* isotherms for the MO-naphthoquinone and MO-ferrocene mixed monolayers over a wide range of MO mole fractions. An example of the results obtained for the 1,4-naphthoquinone-based compounds is shown in Fig. 6, where some of *π-A* isotherms are obtained for mixed QE and MO monolayers at different molar ratios of MO (x_{MO}). The isotherms for mixtures of the other 1,4-naphthoquinone compounds look quite similar to the ones presented in Fig. 6.

As with pure compounds, the dominant structure in the mixed films is liquid-expanded, and the collapse pressure does not depend on the monolayer composition at $x_{MO} > 0.9$. However, the collapse pressure decreases as the content of MO in the mixture decreases below this value. Moreover, the monolayer condenses when the MO content in the mixed film decreases. There is a marked plateau corresponding to the transition between liquid-expanded and liquid-condensed structures in mixed films at $x_{MO} < 0.73$.

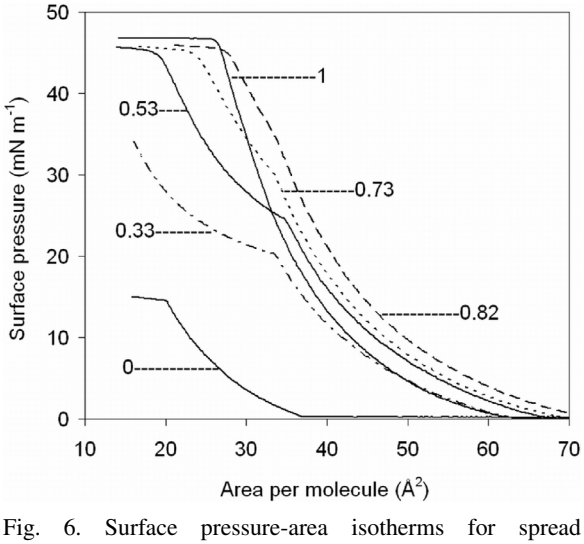

Fig. 6. Surface pressure-area isotherms for spread films of monoolein (MO) and ((Z)-octadec-9-enyl) 1,4-naphthoquinone-2-carboxylate (QE) mixtures for different MO molar fractions (x_{MO}) at the air/water interface at 20 °C.

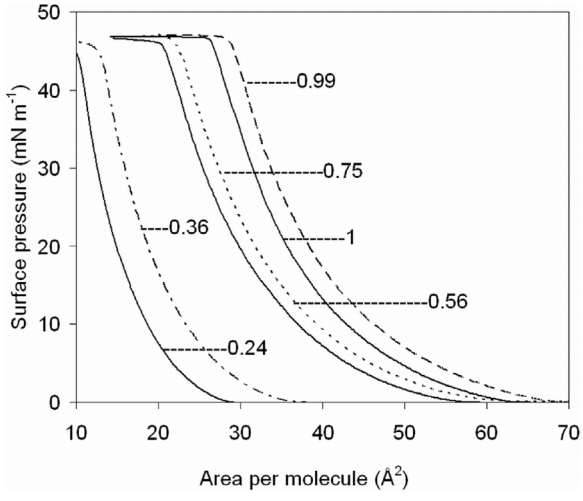

Fig. 7. Surface pressure-area isotherms for spread films of monoolein (MO) and ferrocenylmethyl (*Z*)-octadec-9-enoate (FeE) mixtures for different MO molar fractions (x_{MO}) at the air/water interface at 20 °C.

As discussed above, no *π-A* isotherm for the pure FeE compound could be recorded, as the substance could not be spread quantitatively at the air/water interface. However, when FeE was mixed into the MO monolayer, isotherms could be obtained. At a low molar fraction of FeE in the mixed monolayer, the *π-A* isotherm is actually slightly shifted to higher areas than the corresponding isotherms of MO. From this we can conclude that FeE can be stabilized at the air/water interface by mixing it into the MO monolayer. The shift of the isotherm towards larger area per molecule that occurs when FeE is included in the MO monolayer indicates that the compound is oriented more parallel to the air/water interface. This can also explain the poor spreadability of FeE. The MO monolayer can solubilize up to 76 mol-% of FeE. The collapse pressure observed for the mixed FeE/MO films was similar to that recorded for pure MO, and was practically constant over the studied x_{MO} range, that is, at least for $x_{MO} > 0.24$ (Fig. 7). However, for mixed monolayers with all the other derivatives, the collapse pressure decreases with x_{MO}. This is in line with the data reported by Sanchez *et al.* [41], where the collapse pressure also was found to be independent of the composition of MO-monostearin mixed monolayers.

For the process of mixing, the excess area A_{exc} of mixing can be evaluated directly from the *π-A* isotherms, $A_{exc} = A - (x_1A_1 + x_2A_2)$, where x_i and A_i are the molar fraction in the mixed monolayer and

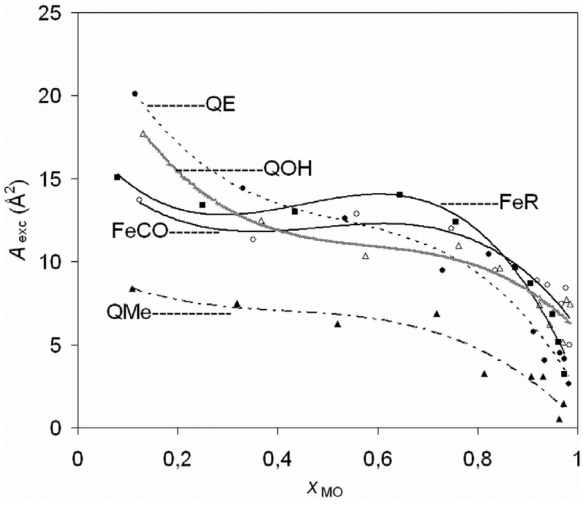

Fig. 8. Surface area excess, A_{exc}, at π = 10 mN m^{-1} for the mixtures of monoolein with the synthesized derivatives *versus* the molar fraction of monoolein at 20 °C.

the molecular area of each component, respectively. For ideal mixing, A_{exc} = 0. The same results are obtained if the lipids are completely immiscible, thus forming separated domains [44]. If one of the components, say component 2, forms an unstable monolayer, then the value of A_2 obtained from the isotherm of the pure substance is underestimated. The excess area in this case, therefore, will be positive, even if the substances form an ideal mixture or if they separate in immiscible domains. From the results and discussion given above we find it likely that all our new derivatives give an apparently larger area when mixed with MO. This makes thorough thermodynamic analysis difficult. Therefore, we have plotted only the calculated A_{exc} values as such and will discuss these data qualitatively.

The calculated values of A_{exc} for mixed films of MO and the derivatives synthesized are shown *versus* molar fraction of MO in Fig. 8. The data are taken at a surface pressure π = 10 mN m^{-1}. For all the derivatives, mixing with MO leads to a positive value of A_{exc}. Thus, we conclude that they do not exhibit ideal solution behavior. The positive value suggests a stabilization of the derivatives as they are mixed into the MO film. When comparing the data for the different derivatives, we note that they are quite similar, but with the exception of QMe. For this compound, the excess area is almost constant at all concentrations and significantly lower than for the other compounds. That is to say that this compound exhibits better solubility in the MO monolayer. For all derivatives, A_{exc} increases with decreasing x_{MO}, while at x_{MO} close to 0.5, A_{exc} is fairly independent of x_{MO}. We can conclude that the mixed film is more stable than the monolayers of the individual derivatives.

Conclusion

The two-dimensional self-assembly of the novel synthesized ferrocene- and 1,4-naphthoquinone-based compounds and their mixtures with monoolein at the air/water interface was studied using the Langmuir film balance technique.

It was found that the head group as well as the positioning of the alkyl chain with respect to the head group can strongly affect the π-*A* isotherm at the air/water interface. Naturally, the type of alkyl chain will also affect the interfacial properties, *e. g.* the collapse pressure. This is in accordance with the reported data for vitamins K_1 (phylloquinone) and K_2 (menaquinone 4) monolayers [45], where the authors found that the collapse pressure for vitamin K_2 is lower because of the double-bonds in the alkyl chain. Furthermore, Deschenaux *et al.* found that ferrocene compounds with two alkyl chains gave more stable monolayers than the corresponding compounds with a single chain [46].

The π-*A* isotherms for the 1,4-naphthoquinone derivatives move towards a smaller area per molecule with increasing temperature. Such a decrease in area per molecule with temperature can be attributed to a loss (desorption) of the spread substance to the subphase due to an increase of its solubility with temperature. The area per molecule for the ferrocene-based compound FeR seems to decrease with increasing temperature, which also can be explained by an increasing loss of material to the sub-phase. In addition, the mixed films of the synthesized compounds with monoolein are more stable than the monolayers of the individual ferrocene- and naphthoquinone-based derivatives.

Acknowledgement

Financial support from The Royal Swedish Academy of Sciences, the Lithuanian Science and Studies foundation and the Swedish Research Council is gratefully acknowledged.

[1] G. L. Gaines, *Insoluble Monolayers at Liquid-Gas Interfaces*, Wiley, New York **1966**.
[2] A. Pockels, *Nature* **1891**, *43*, 437 – 439.
[3] K. Ariga, H. Yuki, J. Kikuchi, O. Dannemuller, A. M. Albrecht-Gary, Y. Nakatani, G. Ourisson, *Langmuir* **2005**, *21*, 4578 – 4583.
[4] I. Panaitov, R. Verger, *Physical Chemistry of Biological Interfaces*, Marcel Dekker, New York **2000**.
[5] B. Piknova, W. R. Scief, B. M. Discher, S. B. Hall, *Biophys. J.* **2001**, *81*, 2172 – 2180.
[6] X. M. Li, J. M. Smaby, M. M. Momsen, H. L. Brockman, Rh. E. Brown, *Biophys. J.* **2000**, *78*, 1921 – 1931.
[7] A. Radhakrishnan, T. G. Anderson, H. M. McConnell, *Proc. Natl. Acad. Sci USA* **2000**, *97*, 12422 – 12427.
[8] J. S. Kim, S. B. Lee, Y. S. Kang, S. M. Park, M. Majda, J. B. Park, *J. Phys. Chem. B* **1998**, *102*, 5794 – 5799.
[9] V. Matti, J. Saily, S. J. Ryhanen, J. M. Holopainen, S. Borocci, G. Maancini, P. K. J. Kinnunen, *Biophys. J.* **2001**, *81*, 2135 – 2143.
[10] K. Hac-Wydro, P. Wydro, P. Dynarowicz-Latka, *J. Colloid Interface Sci*. **2005**, *286*, 504 – 510.
[11] J. Fick, R. Steitz, V. Leiner, S. Tokumitsu, M. Himmelhaus, M. Grunze, *Langmuir* **2004**, *20*, 3848 – 3853.
[12] T. Hianik, P. Vitovic, D. Humenik, S. Yu. Andreev, T. S. Oretskaya, E. A. H. Hall, P. Vadgama, *Bioelectrochemistry* **2003**, *59*, 35 – 40.
[13] M. Cardenas, T. Nylander, B. Jonsson, B. Lindman, *J. Colloid Interface Sci*. **2005**, *286*, 166 – 175.
[14] R. M. Kenn, C. Boehm, A. M. Bibo, I. R. Peterson, H. Moehwald, J. Als-Nielsen, K. Kjaer, *J. Phys. Chem.* **1991**, *95*, 2092 – 2097.
[15] R. Reiter, H. Motschmann, A. Nemetz, W. Knoll, *Langmuir* **1992**, *8*, 1784 – 1788.
[16] D. Honig, D. Mobius, *J. Phys. Chem*. **1991**, *95*, 4590 – 4592.
[17] K. Ekelund, E. Sparr, J. Engblom, S. Engström, H. Wennerström, *Langmuir* **1999**, *20*, 6946 – 6949.
[18] E. Sparr, K. Ekelund, J. Engblom, S. Engström, H. Wennerström, *Langmuir* **1999**, *20*, 6950 – 6955.
[19] J. Majewski, T. L. Kuhl, G. S. Smith, *Biophys. J.* **2001**, *81*, 2707 – 2715.
[20] P. Lehmann, C. Symietz, G. Brezesinski, H. Krass, D. G. Kurth, *Langmuir* **2005**, *21*, 5901 – 5906.
[21] S. L. Keller, T. G. Anderson, H. M. McConnell, *Biophys. J.* **2000**, *79*, 2033 – 2042.
[22] A. Cruz, L. Vazquez, M. Velez, J. Perez-Gil, *Langmuir* **2005**, *21*, 5349 – 5355.
[23] V. Razumas in *Bicontinuous Liquid Crystals* (Eds.: M. L. Lynch, P. T. Spicer), CRC Press Taylor & Francis Group, Boca Raton **2005**, chapter 7, pp. 169 – 211.
[24] J. Barauskas, V. Razumas, T. Nylander, *Chem. Phys. Lipids* **1999**, *97*, 167 – 179.
[25] J. Barauskas, V. Razumas, Z. Talaikytė, A. Bulovas, T. Nylander, D. Tauraitė, E. Butkus, *Chem. Phys. Lipids* **2003**, *123*, 87 – 97.
[26] S. T. Hyde, S. Andersson, B. Ericsson, K. Larsson. *Z. Kristallogr*. **1984**, *168*, 213 – 219.
[27] G. Niaura, Z. Kuprionis, I. Ignatjev, M. Kazemekaite, G. Valincius, Z. Talaikyte, V. Razumas, A. Svendsen, *J. Phys. Chem. B* **2008**, *112*, 4094 – 4101.
[28] E. Butkus, D. Tauraité, J. Barauskas, Z. Talaikyte, V. Razumas, *J. Chem. Res. (S)* **1998**, 722 – 723.
[29] D. F. Evans, H. Wennerstrom, *The Colloidal Domain where Physics, Chemistry, Biology, and Technology Meet*, VSH Publishers, New York **1994**.
[30] F. MacRitchie, *Chemistry at Interfaces*, Academic Press, San Diego **1990**.
[31] J. M. Holopainen, H. L. Brockman, Rh. E. Brown, P. K. J. Kinnunen, *Biophys. J.* **2001**, *80*, 765 – 775.
[32] D. Vollhardt, *Adv. Colloid Interface Sci*. **1993**, *47*, 1 – 23.
[33] D. Vollhardt, T. Kato, M. Kawano, *J. Phys. Chem*. **1996**, *100*, 4141 – 4147.
[34] A. Gericke, J. Simon-Kutscher, H. Hühnerfuss, *Langmuir* **1993**, *9*, 2119 – 2127.
[35] D. Kristensen, T. Nylander, J. T. Rasmussen, M. Paulsson, A. Carlsson, *Langmuir* **1996**, *12*, 5856 – 5862.
[36] I. Pezron, E. Pezron, P. M. Claesson, B. A. Bergenståhl, *J. Colloid Interface Sci*. **1991**, *144*, 449 – 457.
[37] C. C. Sánchez, M. R. R. Niño, J. M. R. Patino, *Colloids Surfaces B: Biointerfaces* **1999**, *12*, 175 – 192.
[38] J. M. R. Patino, R. M. M. Martínez, *J. Colloid Interface Sci*. **1994**, *167*, 150 – 158.
[39] T. R. Jensen, K. Kjaer, P. B. Howes, A. Svendsen, K. Balashev, N. Reitzel, T. Björnholm, *Lipases & Lipids – Structure, Function and Biotechnological Applications*, Crete University Press, Heraklion **2000**.
[40] J. M. R. Patino, C. C. Sánchez, M. R. R. Niño, *Langmuir* **1999**, *15*, 2484 – 2492.
[41] C. C. Sánchez, J. Feria de la Fuente, J. M. R. Patino, *Colloids Surfaces A: Physicochem. Eng. Aspects* **1998**, *143*, 477 – 490.
[42] J. M. R. Patino, M. R. Dominguez, *Colloids Surfaces A: Physicochem. Eng. Aspects* **1993**, *75*, 217 – 228.
[43] J. M. R. Patino, M. R. Dominguez, J. Feria de la Fuente, *J. Colloid Interface Sci*. **1992**, *154*, 146 – 159.
[44] A. W. Adamson, A. P. Gast, *Physical Chemistry of Surfaces*, 6th Ed., Wiley-Interscience, New York **1997**.
[45] A. Barnoski Serfis, R. Katzenberger, *Colloids Surfaces A: Physicochem. Eng. Aspects* **1998**, *138*, 91 – 95.
[46] R. Deschenaux, S. Megert, C. Zumbrunn, J. Ketterer, R. Steigert, *Langmuir* **1997**, *13*, 2363 – 2372.